Superfluid-supersolid phase transition of elongated dipolar Bose-Einstein condensates at finite temperatures

Sánchez-Baena, J.; Pohl, T.; Maucher, F.

DOI
10.1103/PhysRevResearch.6.023183

Publication date
2024

Document Version
Final published version

Published in
Physical Review Research

Superfluid-supersolid phase transition of elongated dipolar Bose-Einstein condensates at finite temperatures

J. Sánchez-Baena [1,*] T. Pohl,[2] and F. Maucher [3,4,†]

[1]*Departamento de Física, Universitat Politècnica de Catalunya, Campus Nord B4-B5, 08034 Barcelona, Spain*

[2]*Institute for Theoretical Physics, Vienna University of Technology (TU Wien), 1040 Vienna, Austria*

[3]*Faculty of Mechanical Engineering, Department of Precision and Microsystems Engineering, Delft University of Technology, 2628 CD Delft, The Netherlands*

[4]*Departamento de Física, Universitat de les Illes Balears and IAC-3, Campus UIB, E-07122 Palma de Mallorca, Spain*

(Received 2 February 2024; accepted 2 May 2024; published 17 May 2024)

We analyze the finite-temperature phase diagram of a dipolar Bose-Einstein condensate confined in a tubular geometry. The effect of thermal fluctuations is accounted for by means of Bogoliubov theory employing the local density approximation. In the considered geometry, the superfluid-supersolid phase transition can be of first and second order. We discuss how the corresponding transition point is affected by the finite temperature of the system.

DOI: 10.1103/PhysRevResearch.6.023183

I. INTRODUCTION

Supersolidity refers to a state of matter that simultaneously features both discrete translational symmetry and a large superfluid fraction and was conceived 50 years ago [1–3]. Dipolar Bose-Einstein condensates (BECs) have emerged as a unique platform for the experimental exploration of such superfluid solids [4–14], and have attracted substantial theoretical interest [7,15–25] in recent years.

The physics of dipolar supersolids is closely connected to quantum fluctuations [26–28] which stabilize the condensate [22–24,29–31] against dipolar collapse [32,33] due to the attractive part of the mean-field interaction between the dipoles of the atoms. The important role of quantum fluctuations results from the anisotropic nature of the long-range dipole-dipole interaction, which also gives rise to a range of pattern formation phenomena [16,19,20,34–40].

For the same reasons, thermal fluctuations [41–45] can also have substantial effects on the phases of dipolar quantum gases, even well below the condensation temperature [46–49]. In particular, recent calculations showed how heating a dipolar superfluid can induce a transition to a solid phase with a periodically modulated condensate density [49].

In this paper, we use Bogoliubov theory [46,47] to numerically study finite-temperature effects on a dipolar BEC with strong transverse confinement in the thermodynamic limit (see Fig. 1). Recent studies of the zero-temperature phase diagram showed that the superfluid-supersolid phase transition of this system can be of first as well as second order [16–18,50,51]. We expand on our previous finding [49] that a supersolid can emerge from a superfluid upon heating a dipolar BEC. We explore how the domains of first- and second-order phase transition deform upon increasing temperature in more depth. However, unlike in [49] we do not fix the chemical potential. It is not immediately obvious how the inclusion of temperature fluctuations affects the order of the phase transition or whether the domain of second order persists. A detailed knowledge of the location of the critical point separating these two domains and its dependence on temperature, condensate density, and scattering length could prove helpful for the design and realization of evaporative cooling protocols to experimentally drive the quantum phase transition in a controlled way.

II. FINITE-TEMPERATURE THEORY

Detailed discussions of finite-temperature effects in dilute Bose-Einstein condensates can be found, e.g., in [41,52–55]. In order to account for the effect of thermal fluctuations in dipolar BECs, we apply Bogoliubov theory and use local density approximation [46,49]. This yields a temperature-dependent extended Gross-Pitaevskii equation (TeGPE) given by

$$\mu\psi(\mathbf{r}) = \left(-\frac{\hbar^2\nabla^2}{2m} + U(\mathbf{r}) + \int d\mathbf{r}' V_{dd}(\mathbf{r}-\mathbf{r}')|\psi(\mathbf{r}')|^2 + \frac{4\pi\hbar^2 a}{m}|\psi(\mathbf{r})|^2 + H_{\rm qu}(\mathbf{r}) + H_{\rm th}(\mathbf{r})\right)\psi(\mathbf{r}) \quad (1)$$

for the condensate wave function $\psi(\mathbf{r})$. Here, μ is the chemical potential, m is the mass, U describes the trapping potential, V_{dd} denotes the dipolar interactions, and a corresponds to the s-wave scattering length. Furthermore, $H_{\rm qu}$ and $H_{\rm th}$ describe effective nonlinear potentials that arise from quantum

*juan.sanchez.baena@upc.edu
†f.maucher@tudelft.nl

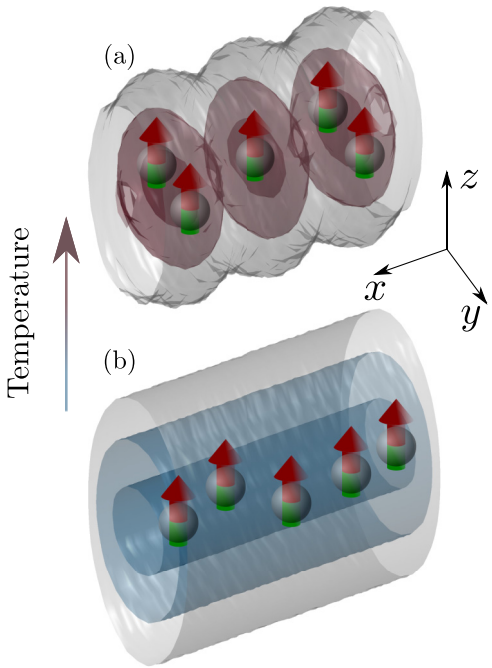

FIG. 1. Schematic representation of the dipolar system in the tubular geometry. Dipoles are polarized along the z axis, while the system extends infinitely along the x axis. By keeping the number of condensed atoms fixed and increasing the temperature, the system transitions from an unmodulated gas (b) to a supersolid (a). The trapping strengths in the y-z plane are given by $\omega_\perp = 0.165\epsilon_d/\hbar$, with $\epsilon_d = \hbar^2/(m(12\pi a_d)^2)$ and a_d denoting the dipolar length.

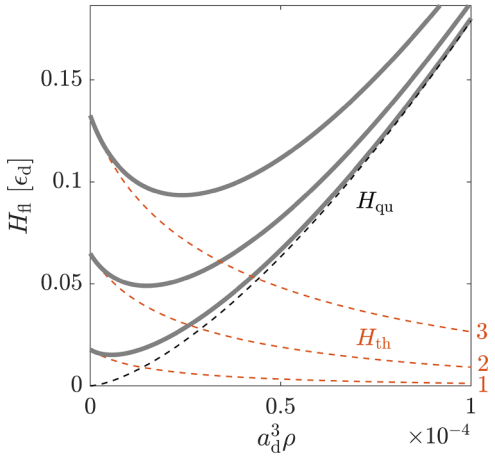

FIG. 2. Density dependence of the energy contributions to the TeGPE from quantum fluctuations, $H_{\rm qu}$, and thermal fluctuations, $H_{\rm th}$, along with the total energy $H_{\rm fl} = H_{\rm th} + H_{\rm qu}$. The results are shown for $a/a_d = 0.7$ and different indicated temperatures $k_BT/\epsilon_d = 1, 2, 3$.

fluctuations and thermal fluctuations, respectively. They are given by

$$H_{\rm qu}(\mathbf{r}) = \frac{32}{3\sqrt{\pi}} g\sqrt{a^3} Q_5(a_d/a)|\psi(\mathbf{r})|^3, \tag{2}$$

$$H_{\rm th}(\mathbf{r}) = \int \frac{d\mathbf{k}}{(2\pi)^3} \frac{1}{(e^{\beta\varepsilon_{\mathbf{k}}} - 1)} \tilde{V}(\mathbf{k}) \frac{\tau_{\mathbf{k}}}{\varepsilon_{\mathbf{k}}(\mathbf{r})}, \tag{3}$$

where $\varepsilon_{\mathbf{k}}(\mathbf{r}) = \sqrt{\tau_{\mathbf{k}}[\tau_{\mathbf{k}} + 2|\psi(\mathbf{r})|^2\tilde{V}(\mathbf{k})]}$ is the Bogoliubov excitation spectrum for a given local density $|\psi(\mathbf{r})|^2$ of the BEC, $\tau_{\mathbf{k}} = \frac{\hbar^2k^2}{2m}$, $\beta = 1/k_BT$, and T denotes temperature. $\tilde{V}(\mathbf{k})$ represents the Fourier transform of the sum of the dipole-dipole interaction and the contact interaction, given by

$$\tilde{V}(\mathbf{k}) = \frac{4\pi\hbar^2 a}{m} + \frac{4\pi\hbar^2 a_d}{m}\left(3\frac{k_z^2}{k^2} - 1\right). \tag{4}$$

The parameter $a_d = mC_{dd}/(12\pi\hbar^2)$ corresponds to the dipolar length, C_{dd} is the strength of the dipolar interaction, and the auxiliary function $Q_5(a_d/a)$ is given by [28]

$$Q_5(a_d/a) = \int_0^1 du\left[1 - \frac{a_d}{a} + 3\left(\frac{a_d}{a}\right)u^2\right]^{5/2}. \tag{5}$$

The term $H_{\rm qu}$ in Eq. (2) that accounts for quantum fluctuations increases with the condensate density and is responsible for arresting collapse as discussed above [22,29,56]. In contrast, thermal fluctuations, as described by Eq. (3), decrease with increasing density ρ [46,49]. Figure 2 illustrates this density dependence and shows that the total fluctuation energy, $H_{\rm fl} = H_{\rm qu} + H_{\rm th}$, features a minimum that shifts towards higher densities with increasing temperature.

The evaluation of Eq. (3) for values of the scattering length that are lower than the dipole length requires special attention since the integrand can in this case become complex. This reflects the instability of a homogeneous condensate, as the excitation spectrum, $\varepsilon_{\mathbf{k}}$, turns imaginary for small momenta and $a < a_d$. The finite transverse size of the partially confined condensate, however, introduces a natural low-momentum cutoff for the considered system. Due to the symmetry of the dipole-dipole interaction, the contribution to the fluctuation energies depends only on k_z and $k_\rho = \sqrt{k_x^2 + k_y^2}$. Considering radial confinement as shown in Fig. 1 with typical system sizes l_y and l_z along the y axis and the z axis, respectively, one obtains lower bounds, $k_z > 2\pi/l_z$ and $k_\rho > 2\pi/l_y$, for both momenta. Here, we use $k_z > 0.007/a_d$ and $k_\rho > 0.017/a_d$ and have checked that a 30% increase of these values does not significantly affect the numerical results.

III. FINITE-TEMPERATURE PHASE DIAGRAM

Equation (1) can be solved numerically by imaginary time evolution to obtain the condensate wave function ψ for a finite temperature, T, and a fixed condensate density or chemical potential, μ. Figure 3 shows the contrast

$$\mathcal{C} = \frac{\rho_{\rm max} - \rho_{\rm min}}{\rho_{\rm max} + \rho_{\rm min}} \tag{6}$$

where $\rho_{\rm max}$ and $\rho_{\rm min}$ denote the maximum and minimum of the axial density $\rho(x) = \int dydz|\psi(\mathbf{r})|^2$ along the x axis. The latter is also used to define the overall axial density $\bar{\rho} = L^{-1}\int_0^L dx\rho(x)$ for a given value of the length L of the simulation box along the x direction.

The axial density contrast vanishes in the superfluid phase, for large ratios a/a_d in Fig. 3, and takes on finite values below a critical value of a/a_d as one enters the solid phase with finite density modulations. For the chosen density of $\bar{\rho}a_d = 4.77$, the zero-temperature simulation yields a

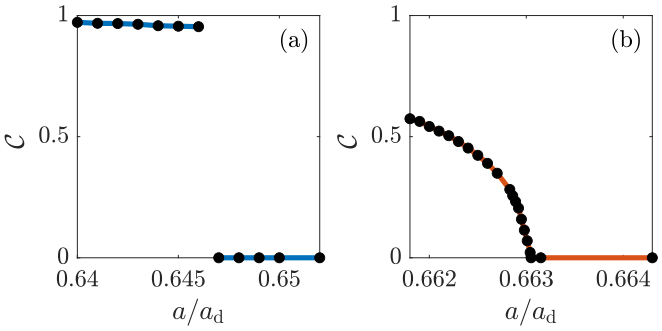

FIG. 3. Contrast of the wave function vs scattering length in a (a) first- and (b) second-order phase transition for $\bar{\rho}a_d = 4.77$ and two different temperatures: $k_BT/\epsilon_d = 0$ (a) and $k_BT/\epsilon_d = 2$ (b).

discontinuous increase of the contrast, characteristic for a first-order phase transition. For a finite temperature of $k_BT/\epsilon_d = 2$, however, one finds a second-order phase transition with a continuous rise of the density contrast. Apart from shifting the transition point, thermal fluctuations, therefore, may also qualitatively affect the fluid-solid phase transition.

Thermal effects are further illustrated in Fig. 4, where we show the contrast across the phase transition as a function of temperature for two different values of the condensate density. In agreement with [49], for the depicted cases we find that heating induces a transition to a density-modulated state. Furthermore, we find that the latter can proceed via a first- or second-order phase transition.

Around the second-order phase transition, one finds moderately modulated states with a density contrast that remains significantly below unity. Concurrently, such states are expected to feature a substantial superfluid fraction [3,57,58] and should, therefore, realize a supersolid. On the other hand, a direct first-order transition from a superfluid to a solid with near unit modulation contrast and no global superfluidity should eventually occur upon decreasing density.

Figure 5 provides a more complete picture of the fluid-solid transition, showing the phase diagram at zero temperature and $k_BT/\epsilon_d = 2$ as a function of the condensate density and the competing interaction strengths. The chosen parameters lie in typical regimes of current experiments, e.g., whereby the temperature corresponds to $T \simeq 87$ nK for a quantum gas of ^{164}Dy atoms. The calculations show that such low

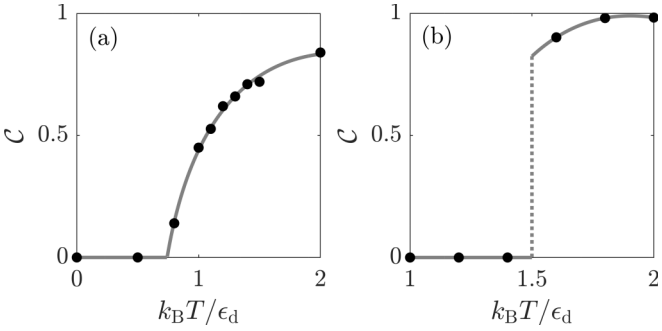

FIG. 4. Contrast of the wave function as a function of temperature for $\bar{\rho}a_d = 6.89$, $a/a_d = 0.676$ (a) and $\bar{\rho}a_d = 4$, $a/a_d = 0.64$ (b). The lines correspond to eye guides.

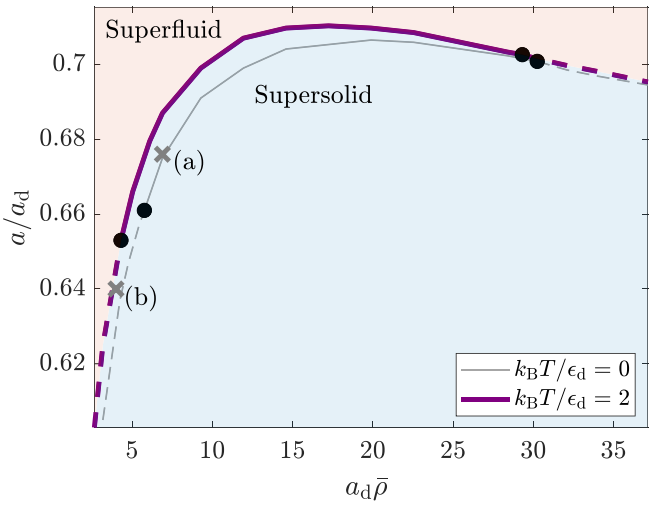

FIG. 5. Superfluid-supersolid phase diagram for $T = 0$ (gray line) and $k_{\rm B}T/\epsilon_{\rm d} = 2$ (purple line). Solid lines show regions where the transition is of continuous or second order whereas dashed lines indicate the presence of a first-order phase transition. The black point marks the low and high density critical point separating regions of first- and second-order phase transitions. The gray crosses refer to Figs. 4(a) and 4(b).

temperatures do not qualitatively alter the phase diagram compared to the ground state behavior of dipolar condensates, discussed recently in [18,50].

As the temperature is increased, the solid-fluid transition line shifts towards larger values of the scattering length a. Starting from the superfluid phase close to the quantum phase transition ($T = 0$) and increasing the temperature, therefore, leads to the emergence of a solid phase upon heating the system regardless of the precise values of the otherwise fixed parameters (i.e., a, a_d, and $\bar{\rho}$). This effect, which has been reported in recent experiments with ^{164}Dy atoms [48,49], can be understood from the characteristic density dependence of the energy, $H_{\rm th}$, of thermal fluctuations shown in Fig. 2. A decreasing energy with increasing density, $|\psi|^2$, implies that $H_{\rm th}[|\psi(\mathbf{r})|]$ acts as a focusing nonlinearity in the generalized GPE [49] and, therefore, tends to support the density-modulated phase. Here, the term "focusing nonlinearity" has been borrowed from optics. The connection to the excitation spectrum can be found by applying linear response theory on an unmodulated stationary solution of the TeGPE, where one finds that $H_{\rm th}$ leads to a roton softening [49] due to $\frac{dH_{\rm th}}{d\bar{\rho}}$ being negative.

We would like to proceed with discussing Fig. 5. To simplify what follows we will roughly distinguish regions of "large" and "small" densities. These regions are separated by the density where the curve of the superfluid-supersolid phase boundary assumes its maximal value of a/a_d. One observes in Fig. 5 a convergence of the phase boundaries for the two considered different temperatures for large densities, which shows again that thermal effects on the phase boundary weaken as the density increases. This can again be readily understood from Fig. 2, which shows that quantum fluctuations yield the dominant contribution to the energy correction $H_{\rm fl}$ at higher densities. While thermal fluctuations always shift

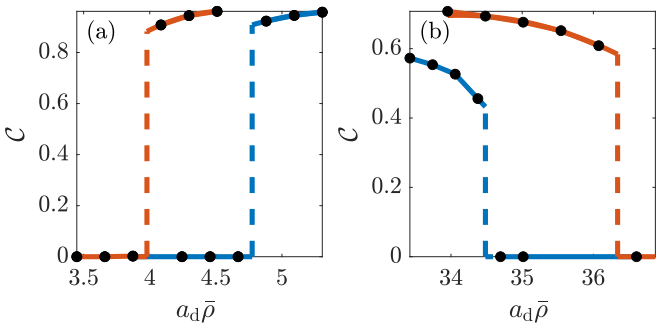

FIG. 6. Contrast $\mathcal{C}$ of the wave function vs axial density in the (a) low density and (b) high density regimes. The value of a/a_{dd} corresponds to $a/a_{dd} = 0.645$ in (a) and to $a/a_{dd} = 0.6965$ in (b).

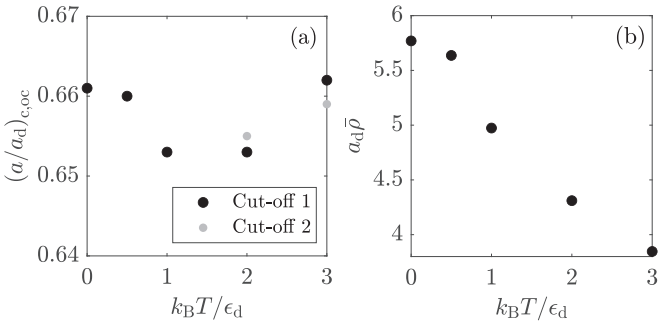

FIG. 7. Scattering length (a) and density (b) of the low density critical point as a function of the temperature. In the plot (a), "Cut-off 1" corresponds to the low-momentum cutoff for the computation of Eq. (3) employed in all the calculations of this paper (i.e., $\{k_z > 0.007/a_d, k_\rho > 0.017/a_d\}$), while "Cut-off 2" corresponds to a 30% increase of these values.

the phase boundary towards larger scattering lengths, a, their effect on the critical density depends on the density itself. At lower densities, where the energy corrections from quantum fluctuations and thermal fluctuations are comparable, the phase boundary is shifted towards lower densities and thereby facilitates the formation of the solid phase. In contrast, at higher densities, where quantum fluctuations dominate the energy correction, $H_{\rm fl}$, a larger temperature requires an increased density to form a modulated state. Yet, heating still facilitates the solid phase, since the critical scattering length decreases with density in this regime (see Fig. 2). This effect is illustrated in Fig. 6, where we show the contrast as a function of $\bar{\rho}$ in the two different density regimes.

We finally discuss the order of the phase transition and how it is affected by thermal fluctuations. At very low densities, the transition is of first-order type but turns into a continuous second-order phase transition with increasing density. Eventually, the phase transition becomes once again discontinuous in the high density regime. This general phenomenology of the quantum phase transition ($T = 0$) [18,50] prevails at finite temperatures, while thermal fluctuations can shift the critical points at which the order of the phase transition changes.

At the low density critical point (see Fig. 5) the change of the critical value of the scattering length [$(a/a_{dd}) = 0.655 \pm 0.005$] is small compared to the experimental resolution for the values considered [see Fig. 7(a)], meaning that, for practical purposes, it can be considered constant with respect to temperature. Its quantitative dependence within the given range is subject to the specific momentum cutoff employed in the computation of Eq. (3), as seen in Fig. 7(a). In contrast to that, one finds a substantial effect on the critical density, which decreases significantly with increasing temperature of the BEC [see Fig. 7(b)]. On the other hand, the shift in the critical point is less pronounced in the high density regime, as can be seen in Fig. 5. This is a consequence of the aforementioned weakening of thermal effects for increasing condensate density. These findings suggest that, from an experimental perspective, the first- or second-order transitions could be probed (aside from finite size effects) by fixing the value of the scattering length, as the value of critical scattering length barely changes with temperature. Then, carrying out an evaporative cooling protocol in the low density regime, where different condensate densities are sampled at different temperatures, leads to either a second-order ($a/a_{dd} > 0.66$) or a first-order ($a/a_{dd} < 0.65$) phase transition.

IV. CONCLUSIONS

In our previous work [49], we computed the phase diagram of the dipolar BEC under a tubular confinement for a fixed chemical potential of $\mu/\epsilon_d = 1$. With this paper we aim to provide a useful followup by means of extending to finite temperature published works [18,50] that employ a tighter trap. Therefore, we have used the condensate density as a parameter for the phase diagram instead of fixing the chemical potential and, furthermore, focus the discussion on the order of the fluid-to-supersolid phase transition in terms of scattering length, condensate density, and temperature. In qualitative agreement with [49], we have seen that an increase of temperature at constant condensate density can yield a transition from an unmodulated superfluid to a supersolid, thus impelling the solid-fluid boundaries of the zero-temperature diagram towards larger values of the scattering length. We have also seen how the low density critical point where the fluid-solid transition shifts from first to second order (or vice versa) changes with temperature and that it moves to lower values of the condensate density, thus yielding a range of parameters for which temperature effectively changes the order of the phase transition. We have also shown that the low density critical scattering length remains unchanged up to experimental resolution, meaning that tuning the scattering length can enable a potential experiment to probe the first- or second-order phase boundaries in a controlled way through an evaporative cooling protocol. For a sufficiently large condensate density we enter a regime where quantum fluctuations dominate and thermal effects become small in comparison. As a consequence, the high density critical point experiences a less significant shift than the low density one.

While, in this paper, the emergence of the dipolar supersolid by heating is observed under a constant condensate density as temperature rises, this phenomenology still occurs if the total density is kept constant instead. This is proven by the calculations in [49], which were carried out for a fixed value of the chemical potential. In the thermodynamic

limit, keeping the chemical potential constant within the grand canonical ensemble is equivalent to keeping the total density constant within the canonical ensemble, thus implying that the solidification of the system by an increase of the temperature should still occur for a constant total density.

The role of temperature in dipolar systems still remains a relatively unexplored subject. It remains unclear how temperature will affect the different geometrical phases both in infinite and trapped quasi-two-dimensional dipolar systems [16,19,20] as well as their superfluid properties [59]. Furthermore, improved theoretical calculations for specific geometries where the local density approximation is not necessary could present avenues towards more accurate quantitative predictions that can be compared with future experiments. Similarly, the realization of *ab initio* calculations [25] that are able to fully account for the effect of temperature could help extend the formalism presented in this paper to the high-temperature regime, where the fraction of condensed atoms is small.

ACKNOWLEDGMENTS

This work was supported by the Austrian Science Fund (Grant No. 10.55776/COE1) and the European Union (NextGenerationEU). F.M. acknowledges support from the Ministerio de Economía y Competitividad (AEI/FEDER UE Grant No. PID2021-128910NB-I00) and support from the TU Delft Open Access Fund.

[1] A. F Andreev and I. M. Lifshitz, Quantum theory of defects in crystals, Sov. Phys. Usp. **13**, 670 (1971).

[2] G. V. Chester, Speculations on Bose-Einstein condensation and quantum crystals, Phys. Rev. A **2**, 256 (1970).

[3] A. J. Leggett, Can a solid be "superfluid"? Phys. Rev. Lett. **25**, 1543 (1970).

[4] L. Chomaz, D. Petter, P. Ilzhöfer, G. Natale, A. Trautmann, C. Politi, G. Durastante, R. M. W. van Bijnen, A. Patscheider, M. Sohmen, M. J. Mark, and F. Ferlaino, Long-lived and transient supersolid behaviors in dipolar quantum gases, Phys. Rev. X **9**, 021012 (2019).

[5] F. Böttcher, J.-N. Schmidt, M. Wenzel, J. Hertkorn, M. Guo, T. Langen, and T. Pfau, Transient supersolid properties in an array of dipolar quantum droplets, Phys. Rev. X **9**, 011051 (2019).

[6] L. Tanzi, E. Lucioni, F. Famà, J. Catani, A. Fioretti, C. Gabbanini, R. N. Bisset, L. Santos, and G. Modugno, Observation of a dipolar quantum gas with metastable supersolid properties, Phys. Rev. Lett. **122**, 130405 (2019).

[7] M. Guo, F. Böttcher, J. Hertkorn, J.-N. Schmidt, M. Wenzel, H. P. Büchler, T. Langen, and T. Pfau, The low-energy goldstone mode in a trapped dipolar supersolid, Nature (London) **574**, 386 (2019).

[8] L. Tanzi, S. M. Roccuzzo, E. Lucioni, F. Famà, A. Fioretti, C. Gabbanini, G. Modugno, A. Recati, and S. Stringari, Supersolid symmetry breaking from compressional oscillations in a dipolar quantum gas, Nature (London) **574**, 382 (2019).

[9] G. Natale, R. M. W. van Bijnen, A. Patscheider, D. Petter, M. J. Mark, L. Chomaz, and F. Ferlaino, Excitation spectrum of a trapped dipolar supersolid and its experimental evidence, Phys. Rev. Lett. **123**, 050402 (2019).

[10] L. Tanzi, J. G. Maloberti, G. Biagioni, A. Fioretti, C. Gabbanini, and G. Modugno, Evidence of superfluidity in a dipolar supersolid from nonclassical rotational inertia, Science **371**, 1162 (2021).

[11] D. Petter, A. Patscheider, G. Natale, M. J. Mark, M. A. Baranov, R. van Bijnen, S. M. Roccuzzo, A. Recati, B. Blakie, D. Baillie, L. Chomaz, and F. Ferlaino, Bragg scattering of an ultracold dipolar gas across the phase transition from Bose-Einstein condensate to supersolid in the free-particle regime, Phys. Rev. A **104**, L011302 (2021).

[12] G. Biagioni, N. Antolini, A. Alaña, M. Modugno, A. Fioretti, C. Gabbanini, L. Tanzi, and G. Modugno, Dimensional crossover in the superfluid-supersolid quantum phase transition, Phys. Rev. X **12**, 021019 (2022).

[13] T. Bland, E. Poli, C. Politi, L. Klaus, M. A. Norcia, F. Ferlaino, L. Santos, and R. N. Bisset, Two-dimensional supersolid formation in dipolar condensates, Phys. Rev. Lett. **128**, 195302 (2022).

[14] M. A. Norcia, E. Poli, C. Politi, L. Klaus, T. Bland, M. J. Mark, L. Santos, R. N. Bisset, and F. Ferlaino, Can angular oscillations probe superfluidity in dipolar supersolids? Phys. Rev. Lett. **129**, 040403 (2022).

[15] R. Bombín, J. Boronat, and F. Mazzanti, Dipolar Bose supersolid stripes, Phys. Rev. Lett. **119**, 250402 (2017).

[16] Y.-C. Zhang, F. Maucher, and T. Pohl, Supersolidity around a critical point in dipolar Bose-Einstein condensates, Phys. Rev. Lett. **123**, 015301 (2019).

[17] P. B. Blakie, D Baillie, and S. Pal, Variational theory for the ground state and collective excitations of an elongated dipolar condensate, Commun. Theor. Phys. **72**, 085501 (2020).

[18] P. B. Blakie, D. Baillie, L. Chomaz, and F. Ferlaino, Supersolidity in an elongated dipolar condensate, Phys. Rev. Res. **2**, 043318 (2020).

[19] Y.-C. Zhang, T. Pohl, and F. Maucher, Phases of supersolids in confined dipolar Bose-Einstein condensates, Phys. Rev. A **104**, 013310 (2021).

[20] J. Hertkorn, J.-N. Schmidt, M. Guo, F. Böttcher, K. S. H. Ng, S. D. Graham, P. Uerlings, T. Langen, M. Zwierlein, and T. Pfau, Pattern formation in quantum ferrofluids: From supersolids to superglasses, Phys. Rev. Res. **3**, 033125 (2021).

[21] J. Hertkorn, J.-N. Schmidt, M. Guo, F. Böttcher, K. S. H. Ng, S. D. Graham, P. Uerlings, H. P. Büchler, T. Langen, M. Zwierlein, and T. Pfau, Supersolidity in two-dimensional trapped dipolar droplet arrays, Phys. Rev. Lett. **127**, 155301 (2021).

[22] F. Wächtler and L. Santos, Quantum filaments in dipolar Bose-Einstein condensates, Phys. Rev. A **93**, 061603(R) (2016).

[23] R. N. Bisset, R. M. Wilson, D. Baillie, and P. B. Blakie, Ground-state phase diagram of a dipolar condensate with quantum fluctuations, Phys. Rev. A **94**, 033619 (2016).

[24] D. Baillie, R. M. Wilson, R. N. Bisset, and P. B. Blakie, Self-bound dipolar droplet: A localized matter wave in free space, Phys. Rev. A **94**, 021602(R) (2016).

[25] F. Böttcher, M. Wenzel, J.-N. Schmidt, M. Guo, T. Langen, I. Ferrier-Barbut, T. Pfau, R. Bombín, J. Sánchez-Baena, J. Boronat, and F. Mazzanti, Dilute dipolar quantum droplets beyond the extended Gross-Pitaevskii equation, Phys. Rev. Res. **1**, 033088 (2019).

[26] R. Schützhold, M. Uhlmann, Y. Xu, and U. R. Fischer, Mean-field expansion in Bose-Einstein condensates with finite-range interactions, Int. J. Mod. Phys. B **20**, 3555 (2006).

[27] A. R. P. Lima and A. Pelster, Quantum fluctuations in dipolar Bose gases, Phys. Rev. A **84**, 041604(R) (2011).

[28] A. R. P. Lima and A. Pelster, Beyond mean-field low-lying excitations of dipolar Bose gases, Phys. Rev. A **86**, 063609 (2012).

[29] H. Kadau, M. Schmitt, M. Wenzel, C. Wink, T. Maier, I. Ferrier-Barbut, and T. Pfau, Observing the rosensweig instability of a quantum ferrofluid, Nature (London) **530**, 194 (2016).

[30] M. Schmitt, M. Wenzel, F. Böttcher, I. Ferrier-Barbut, and T. Pfau, Self-bound droplets of a dilute magnetic quantum liquid, Nature (London) **539**, 259 (2016).

[31] H. Saito, Path-integral Monte Carlo study on a droplet of a dipolar Bose-Einstein condensate stabilized by quantum fluctuation, J. Phys. Soc. Jpn. **85**, 053001 (2016).

[32] T. Lahaye, J. Metz, B. Fröhlich, T. Koch, M. Meister, A. Griesmaier, T. Pfau, H. Saito, Y. Kawaguchi, and M. Ueda, *d*-wave collapse and explosion of a dipolar Bose-Einstein condensate, Phys. Rev. Lett. **101**, 080401 (2008).

[33] T. Koch, T. Lahaye, J. Metz, B. Fröhlich, A. Griesmaier, and T. Pfau, Stabilization of a purely dipolar quantum gas against collapse, Nat. Phys. **4**, 218 (2008).

[34] A. Macia, D. Hufnagl, F. Mazzanti, J. Boronat, and R. E. Zillich, Excitations and stripe phase formation in a two-dimensional dipolar Bose gas with tilted polarization, Phys. Rev. Lett. **109**, 235307 (2012).

[35] A. Macia, J. Boronat, and F. Mazzanti, Phase diagram of dipolar bosons in two dimensions with tilted polarization, Phys. Rev. A **90**, 061601(R) (2014).

[36] A. Gallemí and L. Santos, Superfluid properties of a honeycomb dipolar supersolid, Phys. Rev. A **106**, 063301 (2022).

[37] G. Guijarro, G. E. Astrakharchik, and J. Boronat, Ultradilute quantum liquid of dipolar atoms in a bilayer, Phys. Rev. Lett. **128**, 063401 (2022).

[38] G. Guijarro, G. E. Astrakharchik, G. Morigi, and J. Boronat, Self-assembled chains and solids of dipolar atoms in a multilayer, arXiv:2403.14511.

[39] C. Staudinger, D. Hufnagl, F. Mazzanti, and R. E. Zillich, Striped dilute liquid of dipolar bosons in two dimensions, Phys. Rev. A **108**, 033303 (2023).

[40] J. Sánchez-Baena, R. Bombín, and J. Boronat, Ring solids and supersolids in spherical shell-shaped dipolar Bose-Einstein condensates, arXiv:2312.12164.

[41] A. Griffin, Conserving and gapless approximations for an inhomogeneous Bose gas at finite temperatures, Phys. Rev. B **53**, 9341 (1996).

[42] S. Ronen and J. L. Bohn, Dipolar Bose-Einstein condensates at finite temperature, Phys. Rev. A **76**, 043607 (2007).

[43] R. N. Bisset, D. Baillie, and P. B. Blakie, Finite-temperature trapped dipolar Bose gas, Phys. Rev. A **86**, 033609 (2012).

[44] C. Ticknor, Finite-temperature analysis of a quasi-two-dimensional dipolar gas, Phys. Rev. A **85**, 033629 (2012).

[45] K. Pawlowski, P. Bienias, T. Pfau, and K. Rzazewski, Correlations of a quasi-two-dimensional dipolar ultracold gas at finite temperatures, Phys. Rev. A **87**, 043620 (2013).

[46] E. Aybar and M. Ö. Oktel, Temperature-dependent density profiles of dipolar droplets, Phys. Rev. A **99**, 013620 (2019).

[47] S. F. Öztürk, E. Aybar, and M. Ö. Oktel, Temperature dependence of the density and excitations of dipolar droplets, Phys. Rev. A **102**, 033329 (2020).

[48] M. Sohmen, C. Politi, L. Klaus, L. Chomaz, M. J. Mark, M. A. Norcia, and F. Ferlaino, Birth, life, and death of a dipolar supersolid, Phys. Rev. Lett. **126**, 233401 (2021).

[49] J. Sánchez-Baena, C. Politi, F. Maucher, F. Ferlaino, and T. Pohl, Heating a dipolar quantum fluid into a solid, Nat. Commun. **14**, 1868 (2023).

[50] J. C. Smith, D. Baillie, and P. B. Blakie, Supersolidity and crystallization of a dipolar Bose gas in an infinite tube, Phys. Rev. A **107**, 033301 (2023).

[51] T. Ilg and H. P. Büchler, Ground-state stability and excitation spectrum of a one-dimensional dipolar supersolid, Phys. Rev. A **107**, 013314 (2023).

[52] S. Giorgini, L. P. Pitaevskii, and S. Stringari, Thermodynamics of a trapped Bose-condensed gas, J. Low Temp. Phys. **109**, 309 (1997).

[53] H. Shi and A. Griffin, Finite-temperature excitations in a dilute Bose-condensed gas, Phys. Rep. **304**, 1 (1998).

[54] S. C. Cormack and D. A. W. Hutchinson, Finite-temperature dipolar ultracold Bose gas with exchange interactions, Phys. Rev. A **86**, 053619 (2012).

[55] J. Wang, X.-J. Liu, and H. Hu, Ultradilute self-bound quantum droplets in Bose-Bose mixtures at finite temperature, Chin. Phys. B **30**, 010306 (2021).

[56] L. Chomaz, S. Baier, D. Petter, M. J. Mark, F. Wächtler, L. Santos, and F. Ferlaino, Quantum-fluctuation-driven crossover from a dilute Bose-Einstein condensate to a macrodroplet in a dipolar quantum fluid, Phys. Rev. X **6**, 041039 (2016).

[57] N. Sepúlveda, C. Josserand, and S. Rica, Nonclassical rotational inertia fraction in a one-dimensional model of a supersolid, Phys. Rev. B **77**, 054513 (2008).

[58] A. J. Leggett, On the superfluid fraction of an arbitrary many-body system at $t = 0$, J. Stat. Phys. **93**, 927 (1998).

[59] M. A. Norcia, C. Politi, L. Klaus, E. Poli, M. Sohmen, M. J. Mark, R. N. Bisset, L. Santos, and F. Ferlaino, Two-dimensional supersolidity in a dipolar quantum gas, Nature (London) **596**, 357 (2021).